Systems/Circuits

Rapid Developmental Emergence of Stable Depolarization during Wakefulness by Inhibitory Balancing of Cortical Network Excitability

Matthew T. Colonnese
Department of Pharmacology and Physiology, and Institute for Neuroscience, The George Washington University, Washington, DC 20052

The ability to generate behaviorally appropriate cortical network states is central to sensory perception and plasticity, but little is known about the timing and mechanisms of their development. I paired intracellular and extracellular recordings in the visual cortex of awake infant rats to determine the synaptic and circuit mechanisms regulating the development of a key network state, the persistent and stable subthreshold membrane potential (V_m) depolarization associated with wakefulness/alertness in cortical networks, called the "desynchronized" or "activated" state. Current-clamp recordings reveal that the desynchronized state is absent during the first 2 postnatal weeks, despite behavioral wakefulness. During this period, V_m remains at the resting membrane potential >80% of the time, regardless of behavioral state. V_m dynamics during spontaneous or light-evoked activity were highly variable, contained long-duration suprathreshold plateau potentials, and high spike probability, suggesting an unstable and hyperexcitable early cortical network. Voltage-clamp recordings reveal that effective feedforward inhibition is absent at these early ages despite the presence of feedback inhibition. Stable membrane depolarization during wakefulness finally emerges 1–2 d before eye opening and is statistically indistinguishable from that in adults within days. Reduced cortical excitability, fast feedforward inhibition, and the slow cortical oscillation appear simultaneously with stable depolarization, suggesting that an absence of inhibitory balance during early development prevents the expression of the active state and hence a normal wakeful state in early cortex. These observations identify feedforward inhibition as a potential key regulator of cortical network activity development.

Introduction

The primary cellular and network correlate of alert wakefulness in sensory cortex is the "activated" or "desynchronized" state, a relatively stable subthreshold depolarization resulting from balanced excitation and inhibition in recurrent local cortical circuits (Steriade, 2001; Destexhe et al., 2003; Poulet and Petersen, 2008; Constantinople and Bruno, 2011; Haider et al., 2013). The desynchronized state is proposed to be a long-lasting "active" state, originally described as a short-term depolarization alternating with the "down" state in single neurons during slow-wave sleep (Destexhe et al., 2007). Proposed roles for the active state include regulating plasticity, adapting cortical processing to behavioral needs, and increasing the gain and linearity of visual responses (Haider and McCormick, 2009; Harris and Thiele, 2011). While clearly central to adult cortical function, little is known about the relationships among the development of active states and its relationship to cortical desynchronization and the emergence of functional cortical circuits.

Visual activity during development is defined by two broad stages. First, topographic maps and basic response properties are established in part by waves of spontaneous activity transmitted from the retina (Huberman et al., 2008). Second, with the onset of patterned vision, visual experience becomes critical to build higher-order visual response properties such as direction selectivity, acuity, binocularity, and attention (Barnard, 1999; Farroni et al., 2002; Kiorpes, 2006; Maurer et al., 2007; Smith and Trachtenberg, 2007; White and Fitzpatrick, 2007; Leppänen and Nelson, 2009; Espinosa and Stryker, 2012). Electrophysiological studies in both preterm infants and animal models suggest that a minimal component of cortical active states or desynchronization, continuous activity strongly modulated by sleep/wake states, is absent during the first stage and develops during the second. The transition to the second stage occurs at ages equivalent to the human perinatal period (Dreyfus-Brisac and Monod, 1965; Jouvet-Mounier et al., 1970; Gramsbergen, 1976; Frank and Heller, 1997; Golshani et al., 2009; Rochefort et al., 2009; André et al., 2010; Seelke and Blumberg, 2010; Berkes et al., 2011). Infants show signs of alert processing and visual recognition at birth (Colombo, 2001; Daw, 2006), suggesting that basic network mechanisms of alertness/wakefulness are already in place by birth. Detailed developmental trajectories of cortical activity in frontal (Brockmann et al., 2011), somatosensory (Minlebaev et al., 2011), and visual (Colonnese and Khazipov, 2010;

Received Aug. 27, 2013; revised March 7, 2014; accepted March 12, 2014.

Author contributions: M.T.C. designed research; M.T.C. performed research; M.T.C. analyzed data; M.T.C. wrote the paper.

This work was supported by National Institutes of Health/National Eye Institute Grant EY022730. I thank Dr. Marnie A. Phillips for writing and editing assistance.

The authors declare no competing financial interests.

Correspondence should be addressed to Matthew T. Colonnese, 2300 Eye Street, NW, Ross Hall 639, Washington, DC 20052. E-mail: colonnese@gwu.edu.

DOI:10.1523/JNEUROSCI.3659-13.2014

 0270-6474/14/345477-09$15.00/0

Colonnese et al., 2010) regions in rats show that continuous activity with characteristics of cortical desynchronization, such as low-voltage rapid oscillations, are absent until at least the end of the second postnatal week.

Because membrane voltage [membrane potential (V_m)] dynamics have not been extensively examined over these ages, it is unclear how activity patterns observed in immature cortex differ from adult active states, and whether the continuous activity observed in older infants is a mature desynchronized state. Furthermore, the cellular and network mechanisms underlying the development of active states, such as the maturation of recurrent excitatory connections and functional inhibition, are unknown. Here I use whole-cell patch-clamp *in vivo* in a well established model of cortical network development in primary visual cortex (V1) (Colonnese et al., 2010) to quantitatively describe the emergence of cortical desynchronization, and its relationship to the development of cortical active states, network excitability, and inhibitory–excitatory balance.

Materials and Methods

Experimental procedures. All procedures are consistent with National Institutes of Health guidelines and were approved by The George Washington University Institutional Animal Care and Use Committee. Recording methods have been extensively described (Colonnese et al., 2010; Minlebaev et al., 2011). Long–Evans female rats and litters were acquired from Hilltop Lab Animals at postnatal day 4 [P4 (P0, birth)]. Eye opening occurred between P13 and P14. All animals recorded on P13 had closed eyes; one animal that had not opened its eyes by P14 had them manually opened. Under isoflurane anesthesia, the skull was cleaned, plastic bars were placed over the occipital and nasal bones, and they were sealed to the skull with dental cement. Carprofen (5 mg/kg) was used perioperatively as an analgesic. For recording, under isoflurane anesthesia, the animal was placed in a modified stereotaxic frame attached to the head fixation apparatus. The body was supported within a padded enclosure, which was warmed with an electric blanket. Temperature was monitored with a thermocouple placed under the abdomen and maintained at 33–36°C. Movement was detected using a piezo-based detector that was placed under the enclosure, and an electromyographic (EMG) signal was detected by a stainless steel wire placed in the neck and/or facial muscles. The skull above the monocular visual cortex (2.7–3 mm lateral and 0–1 mm rostral to the lambda suture) was thinned, and electrodes were inserted through small holes made by flaking and resecting the dura locally. An extracellular linear multicontact electrode array (NeuroNexus) was inserted within 300 μm horizontally of the patch electrode to record local field potential (LFP) activity. A contact located in layer 4 was used to define the network state and identify local activity patterns. While not necessarily located in the same layer as the whole-cell recording, layer 4 LFPs allow for more consistent definition of the network state, because the development of network activity patterns has been described in greatest detail there (Colonnese and Khazipov, 2010; Colonnese et al., 2010). Extracellular signals were collected at 32 KHz and digitized using the Cheetah (Neuralynx) amplifier and software package. For whole-cell recordings, intracellular solution consisted of the following (in mM):135 potassium methanesulfonate, 2 $MgCl_2$, 0.1 $CaCl_2$ 1 EGTA(K), 2 Na 2ATP, 5 HEPES, and 5 HEPES(Na), pH 7.25 (osmolarity, 270–285 mOsm). Membrane potential values were corrected for liquid junction potentials of +12 mV. Series resistance was <70 MOhm. Only cells with resting membrane potential (V_{rest}) of less than −60 mV and overshooting action potentials were analyzed. Glutamatergic EPSCs were recorded at the reversal potential of the $GABA_A$ receptor-mediated current (−75 mV); presumptive $GABA_A$ receptor-mediated PSCs were recorded at the EPSC reversal potential (0 mV). Whole-cell configuration was achieved under isoflurane anesthesia (1%) vaporized with oxygen, which was immediately removed upon achieving whole-cell access. Animals were considered alert when they showed consistent (>10 s) movement, which was defined as a variable EMG and movement signal, following isoflurane removal. Analysis of wakeful periods was confined to periods of active movement. In animals older than P13, these periods were associated with low-amplitude, high-frequency activity in the LFP. Few neurons were held long enough for the animal to demonstrate quiescent or slow-wave sleep states (defined as the absence of movement for >1 min). A sleep-like "recovery" state could be analyzed in each animal during the 1 min preceding wakefulness. Recovery contained frequent slow waves after P13 and slow activity transients in younger animals, both of which are suppressed by anesthesia (Colonnese and Khazipov; Colonnese et al., 2010), suggesting that this is a natural, sleep-like state. In animals that did sleep, I observed no difference between recovery and "sleep" states. Visual stimuli were provided by a 100 ms whole-field flash (100 lux) every 30 s on a background of low light (<1lux).

Data analysis. Raw traces were analyzed in Clampfit (Molecular Devices) and by custom-developed analysis routines in Matlab (MathWorks). V_{rest} was defined in current-clamp during anesthesia after achieving whole-cell access. Periods of "depolarization" were defined as the time periods in which V_m was >5 mV above V_{rest}. This value was chosen to reflect likely polysynaptic activity, but was below the mean depolarization levels during active states (P13+) or slow activity transients (<P12). "Waking depolarization" was the peak of the V_m distribution during wakefulness minus the peak during anesthesia (V_{rest}). The presence of long-duration "silent periods" was calculated by determining the length of all periods without depolarization, then counting the proportion that was >1 s. The prevalence of "plateau potentials" was calculated as the proportion of time the neuron was in the depolarized state and was also above spike threshold (after spikes were removed). To determine "depolarization instability," periods of quiet were removed and instability was calculated as the σ of a single Gaussian function fit to the V_m distribution. "Spike density" was the number of action potentials per second occurring when the neuron was in the depolarized state. Examples of these operational definitions are shown in Figure 2. For synaptic current analysis (see Fig. 5), the peak current amplitude in response to each visual stimulus during a 1 s poststimulus window was identified for evoked currents. For spontaneous currents, layer 4 LFP deflections of >150 μV were identified, and the peak current within 100 ms following the LFP was used. For peak spontaneous current, the peak amplitude for all currents measured during a 10 min period in the absence of visual stimulation was identified.

Statistical analysis. Parametric analysis was applied for $n > 10$ for all groups and $p > 0.05$ by the Shapiro–Wilk test for normality. The parametric statistical test used was a Student's t test, which was applied to all spontaneous membrane voltage data. The Wilcoxon rank sum test was applied to synaptic current and evoked V_m data. Data are reported as the mean ± SD, unless otherwise noted.

Results

Rapid emergence of cortical desynchronization and active states before eye opening

Whole-cell patch-clamp recordings in current-clamp mode were initiated in rat monocular V1 under anesthesia, allowing the measurement of V_{rest}. Anesthesia was then removed, and the behavioral state was monitored, allowing measurement of V_m dynamics during behavioral wakefulness (Constantinople and Bruno, 2011). Wakeful V_m dynamics are divisible into two clear developmental periods (Figs. 1, 2). In the first period, before P11, wakefulness is characterized by a persistent down-state with V_m near V_{rest} (for examples of network states described, see Fig. 2*A*,*B*). Membrane dynamics in these young pups were similar during natural sleep, anesthesia, and wakefulness. All three consist primarily of long-duration down-states. The continuous alternation between active and down states seen in sleeping adults was not observed in any state (Haider and McCormick, 2009). V_m depolarization at these young ages, whether during sleep or wakefulness, occurs as two kinds of discrete events: (1) short bursts lasting 200–500 ms with no associated LFP oscillation; and (2) slow-activity transients (SATs), 2–10 s depolarizations with associated rapid (20 Hz) oscillations in the LFP (Colonnese and

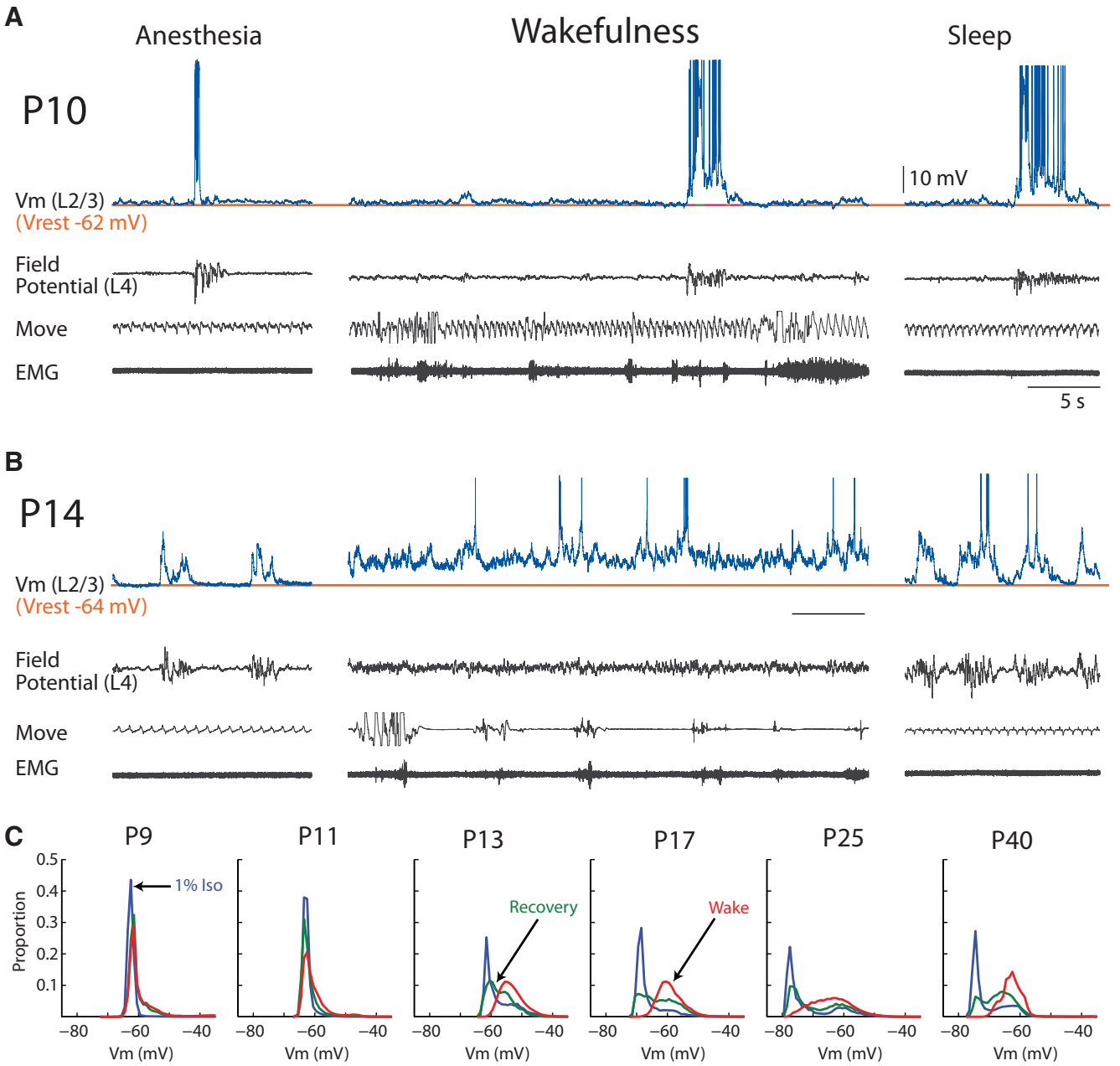

Figure 1. Rapid and simultaneous development of stable membrane depolarization during wakefulness and sleep. ***A***, Intracellular recording of V_m in a layer 2/3 neuron from a P10 rat V1 in the following three states of vigilance: anesthetized (1% isoflurane), awake, and sleeping (quiet/slow-wave sleep). Action potentials are clipped for better resolution. V_{rest} is determined during anesthesia, which is subsequently removed. Simultaneous monitoring of the local field potential in layer 4 (L4), and of movement by piezo-electric and EMG signals is used to determine behavioral state and to identify cortical activity patterns. Note the absence of depolarization during wakefulness and sleep, and the presence of large-amplitude, unstable, discrete events. ***B***, Similar recording at P14. Note stable and persistent depolarization during wakefulness, and up–down state transitions during sleep. ***C***, Histograms of V_m during three vigilance periods: 1% isoflurane anesthesia (blue); 60 s before movement during recovery from isoflurane anesthesia (green); and wakefulness (red). Development of unimodal V_m distribution during wakefulness develops between P11 and P13. Clear separation between active and down states during unconsciousness is visible by P13 but stabilizes over the next week.

Khazipov; Colonnese et al., 2010). Under anesthesia, SATs disappear, leaving only brief bursts of activity (Rochefort et al., 2009). Neither short bursts nor SATs could be classified as cortical active states because (1) their V_m dynamics are unstable, and (2) they frequently include plateau potentials when V_m exceeds the action potential threshold for 10–300 ms (Fig. 2*A*, green boxes). Analysis of the membrane potential distribution between P8 and P11 (Fig. 1*C*) showed no bistability during anesthesia or sleep, as observed in adults by others (Poulet and Petersen, 2008; Constantinople and Bruno, 2011; Haider et al., 2013; Polack et al., 2013). Instead, in all states the V_m distribution includes a single peak at V_{rest} with a long unimodal decay toward depolarized potentials.

Between P11 and P13, the second developmental period started. From this age forward, wakefulness is associated with a persistent depolarizing shift in V_m (Figs. 1*B*, 2*B*) that resembles the "desynchronized" state observed in adult V1 by others (Poulet and Petersen, 2008; Constantinople and Bruno, 2011; Haider et al., 2013; Polack et al., 2013). During anesthesia and natural sleep, V_m alternates between stable depolarization (active states) and V_{rest} (Figs. 1*B*, 2*B*), forming the well described slow oscillation (Steriade et al., 1993). As a result of these changes, V_m bista-

bility during sleep and anesthesia, and a unimodal distribution at depolarized potentials during wakefulness, could be observed in single neurons after P13 (Fig. 1*C*). These changes do not appear to be dependent on pattern vision because they were observed as early as P13, before any pups had opened their eyes.

Quantification of V_m dynamics by age indicates that stable depolarization during wakefulness is adult-like within days of its developmental emergence (Fig. 2*C–H*). The amplitude of the steady depolarization during wakefulness (waking depolarization) from P8 to P11 is only −0.56 to 2.0 mV above V_{rest} measured under anesthesia (mean amplitude, 0.66 ± 0.71 mV). However, from P13 to P25 waking V_m is 8–18 mV above V_{rest} (mean waking V_m, 12.9 ± 2.5 mV; $p = 10^{-18}$), which is similar to adult values. There was no significant effect of age (Fig. 2*C*). The amount of time neurons spend in a depolarized state ("time depolarized"; Fig. 2*D*; 15.9 ± 5.1% at P8–P11 to 92.1 ± 9.5% at P13–P25; $p = 10^{-21}$) and the proportion of down-states of >1 s during wakefulness (silent periods; Fig. 2*E*; 34.1 ± 14.0% to 1.3 ± 4.4%; $p = 10^{-13}$) show that, rather than a slow developmental increase in the time spent depolarized, as soon as the cortex is able to generate a stable depolarization (active state), it can maintain it for long periods during behavioral wakefulness, thereby generating an adult-like desynchronized state.

This reorganization of network activity patterns between P11 and P13 is not a simple increase in excitability or synaptic input. Rather, it appears to be a rebalancing of network excitability, decreasing silent periods but also reducing the total depolarization during network activity. This is most obvious in the presence of plateau potentials, periods of steady V_m depolarization above action potential threshold, which were present only before P13 (for examples of plateau potentials, see Figs. 2*A*, 3*A*, green boxes). From P8 to P11, plateau potentials occupied 10.8 ± 3.5% of the time the neuron was depolarized (Fig. 2*F*). Between P13 and P25, they accounted for only 1.1 ± 1.0% of neuronal depolarization periods ($p = 10^{-17}$). Close examination of the developmental time course shows even further reduction in the prevalence of plateau potentials between P18 and P20 ($p = 0.023$, P13–P18 vs P20–P25).

In the adult, rapid and balanced inhibition counteracts recurrent excitation in cortical networks, stabilizing V_m during active states (Haider and McCormick,

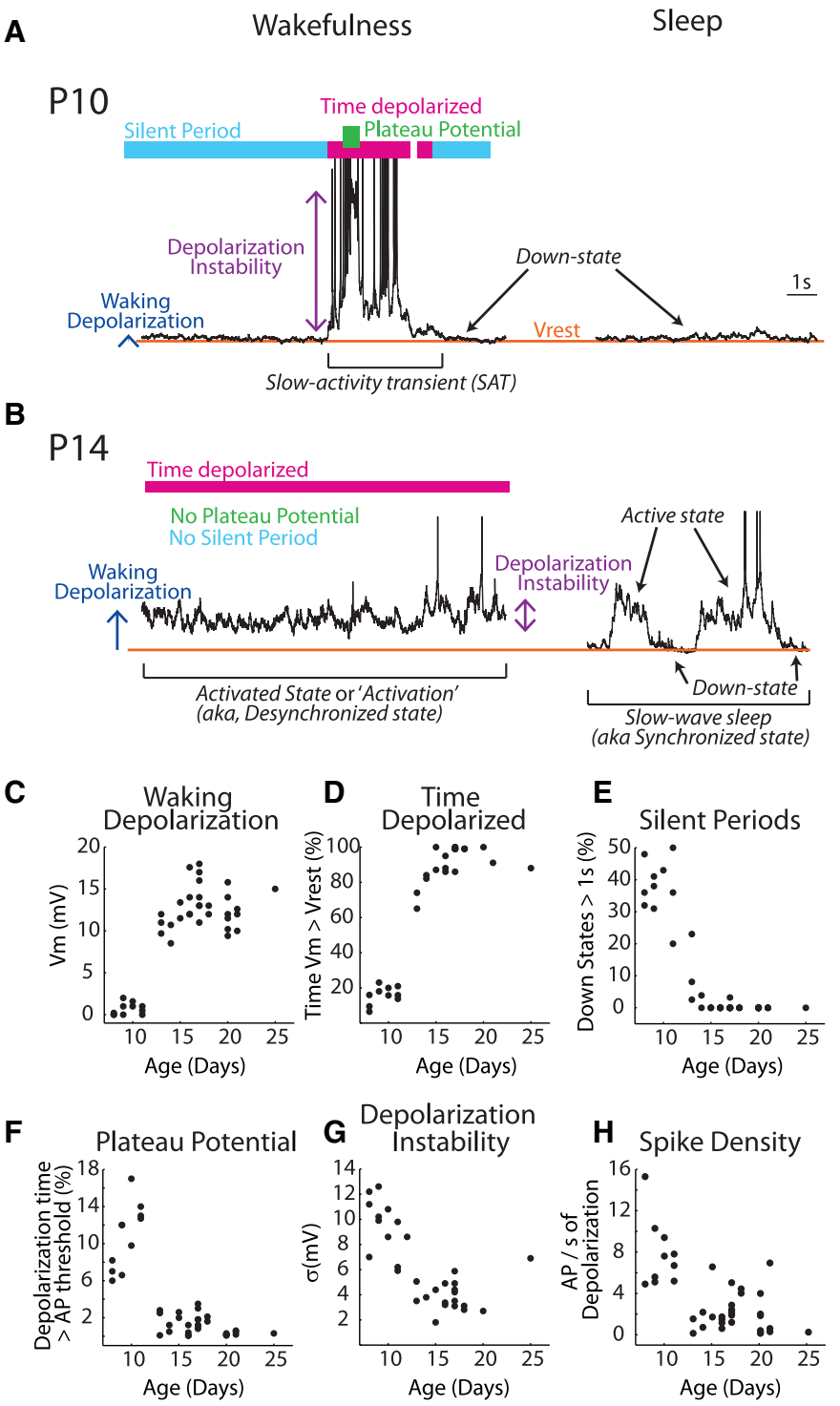

Figure 2. V_m dynamics show rapid development of adult-like depolarization during wakefulness. ***A***, ***B***, Expanded V_m traces from Figure 1 show quantification metrics used during wakefulness (color) and examples of the terms for cortical network states used in the present study (italics). ***C***, Waking depolarization (blue arrows) was quantified as the peak of the V_m distribution (for examples, see Fig. 1*C*) during wakefulness vs V_{rest}. ***D***, Time depolarized (red bars) is the percentage of total time the cell was >5 mV above V_{rest}. ***E***, Silent periods (blue line) are the percentage of periods that the cell spent at V_{rest} that lasted >1 s. ***F***, The incidence of plateau potentials (green box) is the percentage of the time depolarized the cell spent above the action potential (AP) threshold. ***G***, The depolarization instability of depolarization periods (purple arrow) is the σ of a Gaussian distribution fit to the V_m distribution during the time depolarized. ***H***, Spike density is the number of APs per second of depolarization. In line with previous literature, the active state (***B***, right column) is a stable, mostly subthreshold depolarization that occurs during the synchronized state in alternation with down-states (***B***, right column) to form the slow-wave (Haider and McCormick, 2009). The desynchronized state (or activated state) is a persistent depolarization resembling a continuous active state during wakefulness. By these definitions, young animals lack a desynchronized state as well as an active state. Instead, wakefulness (and sleep) is characterized by a persistent down-state, interrupted by large-amplitude unstable activities that spend significant time above the AP threshold. We have previously called these activities SATs (Colonnese and Khazipov, 2010).

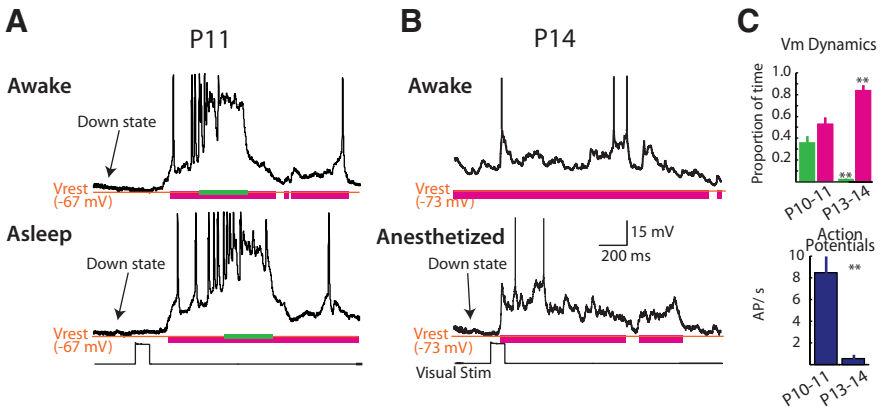

Figure 3. Development of cortical active states attenuates visual responses. ***A***, V_m during evoked activity during wakefulness and sleep before development of cortical active states (P11). Colored lines are as in Figure 1. ***B***, V_m responses after cortical active state development (P14). During wakefulness (top), a brief evoked membrane depolarization rides on a stable membrane depolarization. During unconsciousness (0.5% isoflurane anesthesia), stimulation during down-states can trigger the occurrence of an active state, but does not cause the large, unstable responses of younger animals. ***C***, Quantification of evoked V_m during wakefulness. Top, Proportion of time $V_m >$ AP threshold (plateau potential, green) or >5 mV above V_{rest} (time depolarized, red) following stimulation. Bottom, Number of action potentials during 1 s following stimulation. $^{**}p < 0.01$. Bars indicate the SEM.

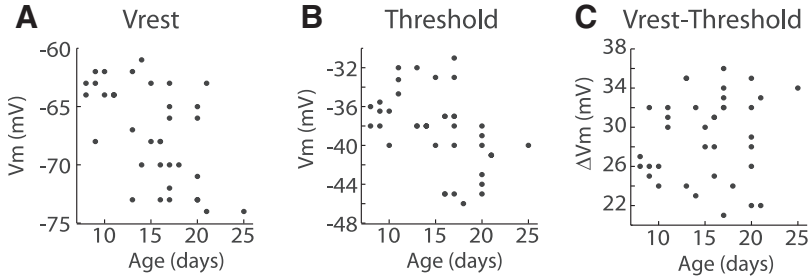

Figure 4. Development of resting membrane potential and action potential threshold. ***A–C***, V_{rest} (***A***), action potential threshold (***B***), and distance between the two (V_{rest} − threshold, ***C***) for each neuron by age.

2009; Renart et al., 2010). The instability of V_m during depolarization periods (depolarization instability), measured as the σ of a single Gaussian fit to the V_m distribution (equivalent to the SD), decreased between P9–P11 and P13–P25 (Fig. 2*G*; from 9.5 ± 2.3 to 3.9 ± 1.2 mV; $p = 10^{-9}$), suggesting inhibitory stabilization of cortical activity. Surprisingly, despite the extensive interneuron development between P13 and P25 (Huang et al., 2007), no changes in V_m stability occurred over these ages (P13–P18 vs P18–P25, $p = 0.6$). The number of action potentials per second of depolarization (spike density), which decreases after eye opening in anesthetized mice (Rochefort et al., 2009), also showed a rapid decrease between P11 and P13 (Fig. 2*H*; depolarization, 7.8 ± 3.2 to 2.1 ± 1.7 spikes/s; $p = 10^{-15}$), providing further evidence of reduced excitability in the network.

Maturation of the cortical network dampens visual responses

I next determined how the changes in cortical network properties leading to the emergence of cortical desynchronization also modulates the V_m dynamics of visual responses. Visual stimulation at P10–P11, before the onset of cortical active states, causes unstable, large-amplitude depolarizations with multiple action potentials riding on a plateau potential during both wakefulness and sleep (Fig. 3*A*). After P12, during wakefulness, the visual response becomes a small depolarizing potential on the background of stable depolarization (Fig. 3*B*, top). If stimulation occurs during a down-state (e.g., during anesthesia or sleep), the visually induced depolarization is likely to be followed by the induction of an up-state (Fig. 3*B*, bottom). These changes result in a decrease in the proportion of time V_m is above the action potential threshold (plateau potential) from 37 ± 12% ($n = 5$) to 1.18 ± 1.62% ($n = 5$; $p = 0.008$) in the 1 s following stimulation (Fig. 3*C*, top), and a decrease in evoked spiking from 8.41 ± 2.88 action potentials in the second following stimulation at P10–P11 to 0.76 ± 0.37 action potentials at P13–P14 ($p = 0.008$; Fig. 3*C*, bottom).

Changes in intrinsic excitability are not associated with the onset of cortical desynchronization

To determine whether changes in V_{rest} or action potential threshold contribute to the emergence of cortical desynchronization, I determined whether they shift rapidly between P11 and P13 (Fig. 4). At P9–P11, V_{rest} measured during anesthesia is between −68 and −62 mV (mean V_{rest}, −63.8 ± 1.7 mV). By P13–P25, the V_{rest} hyperpolarizes slightly, from −74 to −61 mV (mean V_{rest}, −68.7 ± 4.1; $p = 10^{-3}$); however, the change is gradual (Fig. 4*A*), unlike the onset of cortical desynchronization. Action potential threshold hyperpolarized slightly, from between −40 and −32 mV at P9–P11 (mean action potential threshold, −35.9 ± 2.4 mV) and between −46 and −31 mV at P13–P25 (mean action potential threshold, −39.2 ± 4.1; $p = 0.02$), but again the change is gradual (Fig. 4*B*). The total distance between V_{rest} and the action potential threshold is not affected by age (P9–P11, 27.9 ± 3.0 mV; P13–P25, 29.4 ± 4.6 mV; $p = 0.3$; Fig. 4*C*). Thus, while changes in intrinsic excitability likely contribute to the maturation of cortical activity, they are not highly correlated with the emergence of cortical activation between P11 and P13.

Rapid feedforward inhibition emerges with cortical desynchronization and active states

To determine whether changes in thalamic feedforward inputs contribute to the emergence of cortical active states, I measured excitatory and inhibitory currents in voltage-clamp during light-evoked activity in awake animals (Fig. 5). Spontaneous activity was also measured to assay the total synaptic input to each neuron and to determine whether changes in sensory-evoked activity are specific to feedforward circuits.

Strong spontaneous and light-evoked excitatory currents are observed in V1 neurons at all ages (Fig. 5*A*,*B*). Inhibitory currents between P9 and P11, though present during spontaneous activity, are only minimally driven by visual stimulation. As a result, in older animals (P12–P16) the distribution of evoked and spontaneous inhibitory currents largely overlapped, with some tendency for evoked currents to be larger than spontaneous events (Fig. 5*C*). However, in young animals (P9–P11) >90% of evoked inhibitory currents were smaller than the smallest spontaneous current. Excitatory currents showed no developmental change, and spontaneous and evoked excitatory current distributions overlapped at all ages (Fig. 5*C*). To

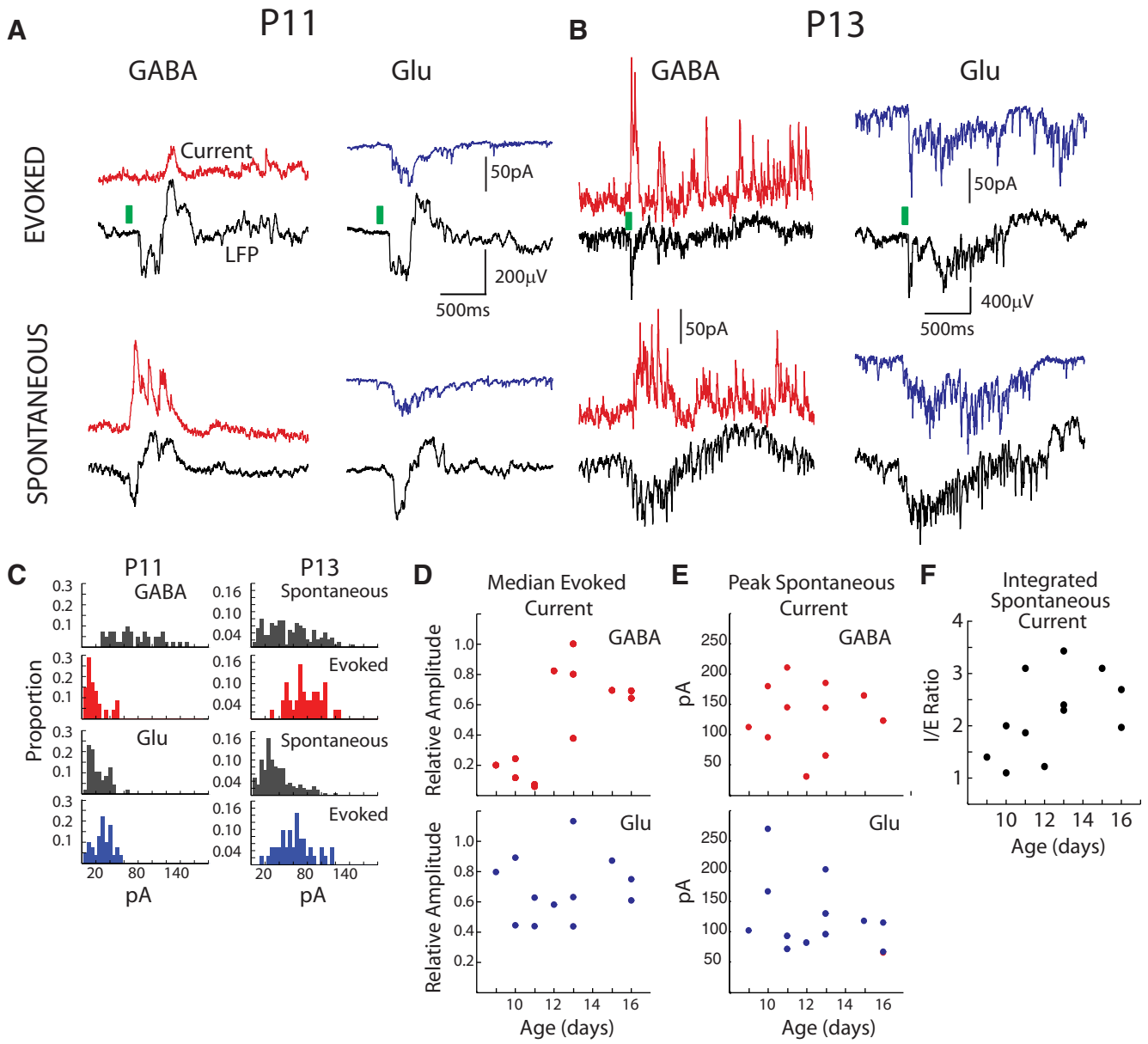

Figure 5. Spontaneous but not light-evoked inhibitory currents in early cortex. ***A***, Light-evoked (top traces) and spontaneous (bottom) synaptic currents and their associated LFP during wakefulness in V1 of P11 rat. Presumptive GABAergic currents (red) and glutamatergic (Glu; blue) currents are recorded for each neuron, and synaptic events with similarly sized LFPs are shown for comparison. Despite large GABAergic currents during spontaneous activity, light (green bars) evokes little synaptic response. ***B***, Same analysis for a neuron from a P13 rat. ***C***, Distribution of spontaneous (gray bars) and evoked (colored bars) currents for GABAergic (top four graphs) and glutamatergic (Glu; bottom four graphs) currents. Example animals from early (P11) and later (P13) ages are shown. ***D***, Median evoked current (relative to peak spontaneous current) for each neuron. GABA currents are shown above in red; glutamate current are shown below in blue. ***E***, Peak spontaneous current used to calculate relative amplitude in ***D***. ***F***, I/E ratio during spontaneous activity for each neuron.

quantify this relationship for each cell, I plotted the median evoked current relative to the peak spontaneous current for each cell. This describes the average visual response as a function of the synaptic capacity of each neuron. For light-evoked excitatory responses, the median-evoked current size does not change over development (Fig. 5*D*, bottom). From P9 to P11, it is 44–89% of the peak spontaneous current (mean current size, 64 ± 20% of peak spontaneous current), and from P12 to P16 it is 44 to 113% (mean current size, 72 ± 23% of peak spontaneous current; $p = 0.88$). In contrast, the median inhibitory response to visual stimulation changes dramatically (Fig. 5*D*, top). At P9–P11, it is only 6–24% of the peak spontaneous current (mean, 14 ± 8%), increasing to 38–102% (mean, 72 ± 23%; $p = 0.0025$) at P12–P16. Peak spontaneous amplitude did not change in the same population (Fig. 5*E*); thus, the change in inhibitory currents is largely due to an increase in the amplitude of evoked currents, which in young animals appears to be far below the total inhibitory synaptic capacity of the cell. This is true neither for excitatory currents at either age or for inhibitory currents after P12. To examine the total current flux transmitted by spontaneous currents, as opposed to their amplitude, I measured the integrated current during spontaneous activity (Fig. 5*F*). This spontaneous ratio of inhibition to excitation (I/E ratio), though it appears to be increasing with age, is not significantly different between P8–P11 and P12–P16 (1.88 ± 0.77 vs 2.80 ± 1.17; $p = 0.16$).

Slower and/or smaller GABAergic currents could contribute to a reduced feedforward inhibitory effectiveness in the V1 of young rats. To examine the precise temporal dynamics of each current in relation to a known input, I measured mean light-

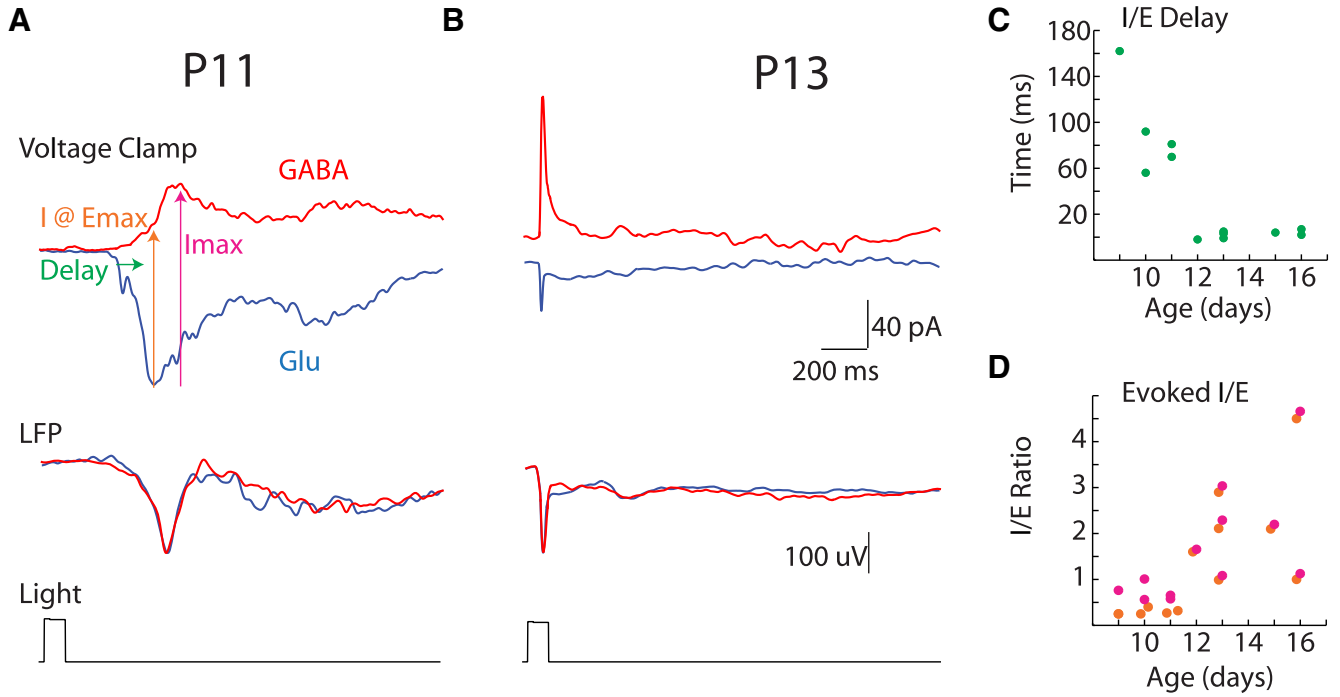

Figure 6. Rapid development of fast feedforward inhibition. ***A***, Mean visually evoked currents for GABA (top red) and glutamate (Glu, top blue), and the mean visually evoked LFP from layer 4 (bottom) for the same neuron for the matched trials from a P11 (left) and P13 (right) rat. ***C***, ***D***, Relationship between excitatory and inhibitory currents is quantified as "Delay," and "I @ Emax," and "Imax," as shown. ***B***, Similar layout for P13. ***C***, Delay between excitatory and inhibitory currents by age. ***D***, Ratio of mean inhibitory current amplitude to mean excitatory current amplitude measured at the peak of the excitatory current (I@Emax, orange) or measured at the peak of each (Imax, red).

evoked currents at each age (Fig. 6). The delay between the 30% rise of the mean excitatory current to the inhibitory current in single neurons shortens substantially between P11 and P12 (Fig. 6*C*), from 56 to 162 ms (mean, 92 ± 41 ms) at P8–P11 to −2 to 7 ms (mean, 2.6 ± 3.2 ms; $p = 0.0025$) at P12–P16. There is a simultaneous increase in the ratio of the peak amplitude of the mean inhibitory to the mean excitatory evoked currents (Fig. 6*D*): from 0.41 to 1.01 (mean, 0.68 ± 0.22) at P8–P11 to 1.01 to 4.66 (mean, 2.26 ± 1.26; $p = 0.0025$) at P12–P16. Because of the longer delay in young animals, the I/E ratio measured at the peak of the excitatory current increased even more dramatically (Fig. 6*D*), from 0.25 to 0.40 (mean, 0.30 ± 0.64) at P9–P11 to 0.99 to 4.51 (mean, 2.17 ± 1.23; $p = 0.0025$) at P12–P16. These data show that the development of fast feedforward inhibition, but not total inhibition, is tightly locked to the maturation of cortical desynchronization and the emergence of active states.

Discussion

The present study has identified a critical developmental checkpoint in sensory cortex, namely, the capacity to maintain stable and persistent activity in the network through balanced excitation and inhibition. It has been suggested that the balanced depolarization during wakefulness, referred to as activation and resulting in the desynchronized state (Steriade and McCarley, 2005), and the up-states occurring during unconsciousness (active states) result from the same network processes; in essence, the desynchronized state is a continuous active state (Destexhe et al., 2007). The simultaneous emergence of both states in my recordings is strong evidence for this. My data further suggest that it is the fundamental ability of cortex to generate balanced and stable depolarization (i.e., the active state), that is the limiting factor in the development of stable depolarization during wakefulness as well as the emergence of true slow-wave sleep. Despite moderate changes in the regulatory components of the sleep/wake cycle and changes in retinal activity during development, my data do not support their involvement in the emergence of cortical desynchronization. The idea that active state development is a limiting step in cortical development clarifies and unites a number of disparate observations of human and animal EEG development. These include the observations that human sleep/wake EEG patterns are reorganized around term (André et al., 2010; Scher, 2011), that EEG infra-slow activities (Tolonen et al., 2007; Colonnese and Khazipov, 2010) and sensory responses (Colonnese et al., 2010) decrease during development, and that neural desynchronization occurs in S1 (Golshani et al., 2009) and V1 (Rochefort et al., 2009) during these early postnatal ages.

Directly measuring intracellular V_m *in vivo* produced multiple results that could not have been predicted from previous extracellular and current recordings. (1) During the early period, wakeful depolarization is not simply smaller than in the adult, and thus below the level of detection; it is in fact not modulated during wakefulness at all. (2) Depolarization during desynchronization is adult like both in duration and amplitude as soon as it is initiated. Thus, the desynchronized state does not develop by stringing together brief active states, elongating immature active states, or by a progressive and graded increase in recurrent excitation and depolarization. (3) While early cortex can produce periods of activity that superficially resemble the active state, this cortical activity is unbalanced and unstable, and thus is unlike the active state described in adults. (4) The key change in cortical network dynamics associated with the onset of cortical desynchronization and active states is a reduction in excitability. Together, this is direct evidence that the limiting factor in the development of cortical active states is not the development of corticocortical excitatory connections, as previously proposed

(Colonnese et al., 2010). In fact, depolarization during spontaneous activity is sufficiently strong to drive and maintain neurons above action potential threshold. Additionally, neither an increase in excitatory spontaneous synaptic potentials nor a steady increase in the amplitude of depolarization during periods when the cortex is active was observed in the period leading up to the onset of active states, either of which might implicate an increase in excitatory synaptic connections in their developmental initiation. Instead, the deficiency of early circuits appears to lie in the opposite direction: insufficient inhibition to balance excitatory inputs that are already in place. As described in isolated cortical slices, unbalanced excitation limits the self-propagating activity of the slow oscillation, shortening active states and increasing the duration of down-states (Sanchez-Vives et al., 2010), potentially contributing to the shortening of down-states observed here. Previous work in the somatosensory cortex *in vivo* showed that a similar development of rapid inhibition is correlated with the elimination of early gamma oscillations (Minlebaev et al., 2011). However, the relative roles of feedforward versus feedback inhibition were not quantified, and it was unclear whether this inhibitory development simply eliminated an immature activity pattern or also actively induced a mature activity pattern. Here, I provide evidence in V1 that thalamic, or feedforward, inhibition develops later than intracortical, or feedback, inhibition. At the same time, cortex acquires the capacity to generate the balanced subthreshold depolarization necessary for balanced depolarization during wakefulness as well as the active state during sleep. The mechanism of this feedforward inhibitory development is unclear, but a similar development has been described in S1 *in vitro*, where experience-dependent strengthening of thalamic synapses on fast-spiking interneurons drives the emergence of feedforward inhibition (Daw et al., 2007; Chittajallu and Isaac, 2010). The striking similarity to our current observations suggests that a similar process occurs in V1, albeit 4 d later.

After its emergence, the amplitude, duration, and stability of cortical depolarization during wakefulness was remarkably consistent between P13 and 25. This occurs despite the significant subsequent increase in synaptic density (Blue and Parnavelas, 1983), and the massive experience-dependent reorganization of the structure and function of glutamatergic and GABAergic synapses (Quinlan et al., 1999; Yoshii et al., 2003; Levelt and Hübener, 2012). This stability of cortical depolarization parameters, despite such significant synaptic development, suggests a strong homeostatic regulation that maintains the active-state depolarization within a narrow window (Maffei et al., 2012). It is surprising to observe mature active states before visual experience and the refinement of long-range cortical connectivity, because depolarization during active states has been proposed to transiently link relevant circuits as a mechanism for visual memory, attention, and developmental plasticity (Berkes et al., 2011; Harris and Thiele, 2011; Aton et al., 2013). One possibility is that while the specific intracortical connections supporting the active state are refined during developmental plasticity, they maintain a constant level of depolarization. This hypothesis is supported by recent evidence showing consistent connection probability but increasing refinement of pyramidal cell connectivity in rodent V1 during the time period examined here (Ko et al., 2013).

The lack of an active state or desynchronized state during the developmental equivalent of the fetal period in humans provides more evidence that cortical circuit development can be divided into two clear periods. First, during initial formation of topographic maps, activity is provided by the periphery, generated by specialized transient circuits that spontaneously cause bursting activity (Blankenship and Feller, 2010). So as not to compete with this critical retinal input, spontaneous activity within thalamic cortex is minimized, while the transmission of this input is maximized by delaying and minimizing feedforward inhibition. The suprathreshold depolarization and extensive synchronization brought about by these network properties is expected to support maximal depolarization, and hence plasticity, of the relevant inputs. However, there is likely a tradeoff between plasticity and the capacity for alert sensory processing. A major role for the development of feedforward inhibition is to remove the effects of shared inputs in the cortical network, allowing for the generation of desynchronization in the cortical circuit (Renart et al., 2010). This developmental step probably allows for alert sensory processing and further plasticity based on the fine structure of the visual world. Inhibitory development is likely not the sole contributor to these changes, but rather one component in a multifactoral maturational event that includes changes in retinal and thalamic circuits as well as ascending neuromodulatory development (Bickford et al., 2010; Colonnese and Khazipov, 2012). Determining how this critical checkpoint is controlled will increase our understanding of how cortical activity is matched to the changing needs of the developing animal, and may provide novel clues for neurodevelopmental disorders that involve deficient maturation of attention, cognition, or sensory processing (Gogolla et al., 2009).

References

André M, Lamblin MD, d'Allest AM, Curzi-Dascalova L, Moussalli-Salefranque F, S Nguyen The T, Vecchierini-Blineau MF, Wallois F, Walls-Esquivel E, Plouin P (2010) Electroencephalography in premature and full-term infants. Developmental features and glossary. Neurophysiol Clin 40:59–124. CrossRef Medline

Aton SJ, Broussard C, Dumoulin M, Seibt J, Watson A, Coleman T, Frank MG (2013) Visual experience and subsequent sleep induce sequential plastic changes in putative inhibitory and excitatory cortical neurons. Proc Natl Acad Sci U S A 110:3101–3106. CrossRef Medline

Barnard KE (1999) Beginning rhythms: the emerging process of sleep wake behaviors and self-regulation. Seattle, WA: NCAST, University of Washington.

Berkes P, Orbán G, Lengyel M, Fiser J (2011) Spontaneous cortical activity reveals hallmarks of an optimal internal model of the environment. Science 331:83–87. CrossRef Medline

Bickford ME, Slusarczyk A, Dilger EK, Krahe TE, Kucuk C, Guido W (2010) Synaptic development of the mouse dorsal lateral geniculate nucleus. J Comp Neurol 518:622–635. CrossRef Medline

Blankenship AG, Feller MB (2010) Mechanisms underlying spontaneous patterned activity in developing neural circuits. Nat Rev Neurosci 11:18–29. CrossRef Medline

Blue ME, Parnavelas JG (1983) The formation and maturation of synapses in the visual cortex of the rat. II. quantitative analysis. J Neurocytol 12:697–712. CrossRef Medline

Brockmann MD, Pöschel B, Cichon N, Hanganu-Opatz IL (2011) Coupled oscillations mediate directed interactions between prefrontal cortex and hippocampus of the neonatal rat. Neuron 71:332–347. CrossRef Medline

Chittajallu R, Isaac JT (2010) Emergence of cortical inhibition by coordinated sensory-driven plasticity at distinct synaptic loci. Nat Neurosci 13:1240–1248. CrossRef Medline

Colombo J (2001) The development of visual attention in infancy. Annu Rev Psychol 52:337–367. CrossRef Medline

Colonnese M, Khazipov R (2012) Spontaneous activity in developing sensory circuits: implications for resting state fMRI. Neuroimage 62:2212–2221. CrossRef Medline

Colonnese MT, Khazipov R (2010) "Slow activity transients" in infant rat visual cortex: a spreading synchronous oscillation patterned by retinal waves. J Neurosci 30:4325–4337. CrossRef Medline

Colonnese MT, Kaminska A, Minlebaev M, Milh M, Bloem B, Lescure S, Moriette G, Chiron C, Ben-Ari Y, Khazipov R (2010) A conserved

switch in sensory processing prepares developing neocortex for vision. Neuron 67:480–498. CrossRef Medline
Constantinople CM, Bruno RM (2011) Effects and mechanisms of wakefulness on local cortical networks. Neuron 69:1061–1068. CrossRef Medline
Daw MI, Ashby MC, Isaac JT (2007) Coordinated developmental recruitment of latent fast spiking interneurons in layer IV barrel cortex. Nat Neurosci 10:453–461. CrossRef Medline
Daw N (2006) Visual development. New York: Springer.
Destexhe A, Rudolph M, Paré D (2003) The high-conductance state of neocortical neurons in vivo. Nat Rev Neurosci 4:739–751. CrossRef Medline
Destexhe A, Hughes SW, Rudolph M, Crunelli V (2007) Are corticothalamic 'up' states fragments of wakefulness? Trends Neurosci 30:334–342. CrossRef Medline
Dreyfus-Brisac C, Monod N (1965) Sleep of premature and full-term neonates—a polygraphic study. Proc R Soc Med 58:6–7. Medline
Espinosa JS, Stryker MP (2012) Development and plasticity of the primary visual cortex. Neuron 75:230–249. CrossRef Medline
Farroni T, Csibra G, Simion F, Johnson MH (2002) Eye contact detection in humans from birth. Proc Natl Acad Sci U S A 99:9602–9605. CrossRef Medline
Frank MG, Heller HC (1997) Development of diurnal organization of EEG slow-wave activity and slow-wave sleep in the rat. Am J Physiol 273:R472–R478. Medline
Gogolla N, Leblanc JJ, Quast KB, Südhof TC, Fagiolini M, Hensch TK (2009) Common circuit defect of excitatory-inhibitory balance in mouse models of autism. J Neurodev Disord 1:172–181. CrossRef Medline
Golshani P, Gonçalves JT, Khoshkhoo S, Mostany R, Smirnakis S, Portera-Cailliau C (2009) Internally mediated developmental desynchronization of neocortical network activity. J Neurosci 29:10890–10899. CrossRef Medline
Gramsbergen A (1976) The development of the EEG in the rat. Dev Psychobiol 9:501–515. CrossRef Medline
Haider B, McCormick DA (2009) Rapid neocortical dynamics: cellular and network mechanisms. Neuron 62:171–189. CrossRef Medline
Haider B, Häusser M, Carandini M (2013) Inhibition dominates sensory responses in the awake cortex. Nature 493:97–100. CrossRef Medline
Harris KD, Thiele A (2011) Cortical state and attention. Nat Rev Neurosci 12:509–523. CrossRef Medline
Huang ZJ, Di Cristo G, Ango F (2007) Development of GABA innervation in the cerebral and cerebellar cortices. Nat Rev Neurosci 8:673–686. CrossRef Medline
Huberman AD, Feller MB, Chapman B (2008) Mechanisms underlying development of visual maps and receptive fields. Annu Rev Neurosci 31:479–509. CrossRef Medline
Jouvet-Mounier D, Astic L, Lacote D (1970) Ontogenesis of the states of sleep in rat, cat, and guinea pig during the first postnatal month. Dev Psychobiol 2:216–239. Medline
Kiorpes L (2006) Visual processing in amblyopia: animal studies. Strabismus 14:3–10. CrossRef Medline
Ko H, Cossell L, Baragli C, Antolik J, Clopath C, Hofer SB, Mrsic-Flogel TD (2013) The emergence of functional microcircuits in visual cortex. Nature 496:96–100. CrossRef Medline
Leppänen JM, Nelson CA (2009) Tuning the developing brain to social signals of emotions. Nat Rev Neurosci 10:37–47. CrossRef Medline
Levelt CN, Hübener M (2012) Critical-period plasticity in the visual cortex. Annu Rev Neurosci 35:309–330. CrossRef Medline
Maffei A, Bucher D, Fontanini A (2012) Homeostatic plasticity in the nervous system. Neural Plast 2012:913472. CrossRef Medline
Maurer D, Mondloch CJ, Lewis TL (2007) Effects of early visual deprivation on perceptual and cognitive development. Prog Brain Res 164:87–104. CrossRef Medline
Minlebaev M, Colonnese M, Tsintsadze T, Sirota A, Khazipov R (2011) Early gamma oscillations synchronize developing thalamus and cortex. Science 334:226–229. CrossRef Medline
Polack PO, Friedman J, Golshani P (2013) Cellular mechanisms of brain state-dependent gain modulation in visual cortex. Nat Neurosci 16:1331–1339. CrossRef Medline
Poulet JF, Petersen CC (2008) Internal brain state regulates membrane potential synchrony in barrel cortex of behaving mice. Nature 454:881–885. CrossRef Medline
Quinlan EM, Philpot BD, Huganir RL, Bear MF (1999) Rapid, experience-dependent expression of synaptic NMDA receptors in visual cortex in vivo. Nat Neurosci 2:352–357. CrossRef Medline
Renart A, de la Rocha J, Bartho P, Hollender L, Parga N, Reyes A, Harris KD (2010) The asynchronous state in cortical circuits. Science 327:587–590. CrossRef Medline
Rochefort NL, Garaschuk O, Milos RI, Narushima M, Marandi N, Pichler B, Kovalchuk Y, Konnerth A (2009) Sparsification of neuronal activity in the visual cortex at eye-opening. Proc Natl Acad Sci U S A 106:15049–15054. CrossRef Medline
Sanchez-Vives MV, Mattia M, Compte A, Perez-Zabalza M, Winograd M, Descalzo VF, Reig R (2010) Inhibitory modulation of cortical up states. J Neurophysiol 104:1314–1324. CrossRef Medline
Scher MS (2011) Ontogeny of EEG sleep from neonatal through infancy periods. Handb Clin Neurol 98:111–129. CrossRef Medline
Seelke AM, Blumberg MS (2010) Developmental appearance and disappearance of cortical events and oscillations in infant rats. Brain Res 1324:34–42. CrossRef Medline
Smith SL, Trachtenberg JT (2007) Experience-dependent binocular competition in the visual cortex begins at eye opening. Nat Neurosci 10:370–375. CrossRef Medline
Steriade M (2001) Impact of network activities on neuronal properties in corticothalamic systems. J Neurophysiol 86:1–39. Medline
Steriade M, McCarley RW (2005) Brain control of wakefulness and sleep. New York: Springer.
Steriade M, Nuñez A, Amzica F (1993) A novel slow (<1 Hz) oscillation of neocortical neurons in vivo: depolarizing and hyperpolarizing components. J Neurosci 13:3252–3265. Medline
Tolonen M, Palva JM, Andersson S, Vanhatalo S (2007) Development of the spontaneous activity transients and ongoing cortical activity in human preterm babies. Neuroscience 145:997–1006. CrossRef Medline
White LE, Fitzpatrick D (2007) Vision and cortical map development. Neuron 56:327–338. CrossRef Medline
Yoshii A, Sheng MH, Constantine-Paton M (2003) Eye opening induces a rapid dendritic localization of PSD-95 in central visual neurons. Proc Natl Acad Sci U S A 100:1334–1339. CrossRef Medline